

KERNFORSCHUNGSZENTRUM

KARLSRUHE

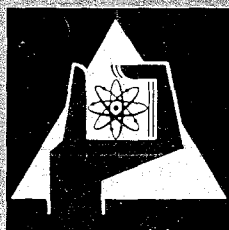
Juli 1967

KFK 602
SM 96/104

Institut für Angewandte Kernphysik

A Review of Scattering Law Studies for Moderators

W. Gläser



GESELLSCHAFT FÜR KERNFORSCHUNG M. B. H.

KARLSRUHE



KERNFORSCHUNGSZENTRUM KARLSRUHE

Juli 1967

KFK 602

SM 96/104

Institut für Angewandte Kernphysik

A Review of Scattering Law Studies
for Moderators

W. Gläser

Gesellschaft für Kernforschung m.b.H. Karlsruhe

INTERNATIONAL ATOMIC ENERGY AGENCY
SYMPOSIUM ON NEUTRON THERMALIZATION
AND REACTOR SPECTRA

Ann Arbor, USA, 17-21 July 1967

SM 62/1

A REVIEW OF SCATTERING LAW STUDIES
FOR MODERATORS

W. Gläser
Kernforschungszentrum Karlsruhe

I. Introduction

The problem we have to deal with is the scattering of neutrons with an energy below a few eV, in condensed matter. In the last two decades it has been proven that neutrons of such energy are extremely versatile probes for studying the details of the structure and dynamics of atomic many particle systems, and neutron scattering measurements have delivered new insight into this behaviour. Also the general theoretical picture describing the neutron scattering process has been developed and has been successfully used in many cases to explain experimental results. We have to restrict ourselves here on a small part of this work, namely, on the investigation of materials which are of interest as reactor moderators.

As an introduction it may be worthwhile to recall the basic formulae. In the first Born approximation, using the Fermi pseudopotential, the double differential scattering cross section can be written

$$\frac{d^2\sigma}{d\Omega dE} = \frac{k}{k_0} \sum_{i,f} p_i \left| \langle f | \sum_n b_n e^{i\vec{k}_f \cdot \vec{r}_n} | i \rangle \right|^2 \delta(E - E_0 + \hbar\omega)$$

$$\hbar\omega = E_f - E_i, \quad \hbar\vec{k} = \hbar(\vec{k}_0 - \vec{k}), \quad (1)$$

where i, f are the initial and final state of the scatterer, $E_{i, f}$ the corresponding energies, p_i is the population of the initial state and b_n is the bound scattering amplitude of the n -th nucleus, \vec{k}_0, \vec{k} are the wave vectors of the incident and scattered neutron and E_0, E the corresponding energies. For scatterers consisting of a single atomic species (1) can be written

$$\frac{d^2\sigma}{d\Omega dE} = \frac{\sigma_b}{4\pi} \frac{k}{k_0} S(\vec{k}, \omega) \quad (2)$$

where σ_b is the bound scattering cross section.

$S(\vec{k}, \omega)$ depends only on the structure and dynamics of the scatterer and is called the scattering law of the system or its dynamical structure factor. From (2) it follows that $S(\vec{k}, \omega)$ can be derived directly from an absolute determination of the double differential cross section.

If we further restrict to isotropic materials, which in general includes all moderators, (1) is often rewritten in the form

$$\sigma(E_0 \rightarrow E, \cos \mathcal{D}) = \frac{\sigma_b}{2k_B T} \sqrt{\frac{E}{E_0}} e^{-B/2} S(\alpha, B) = \frac{1}{2k_B T} \sqrt{\frac{E}{E_0}} e^{-B/2} \left\{ \sigma_b S_s(\alpha, B) + \sigma_c S_d(\alpha, B) \right\}$$

$$\alpha = \frac{m(E_0 + E - 2\sqrt{E_0 E} \cos \mathcal{D})}{M k_B T}, \quad B = \frac{E - E_0}{k_B T} \quad (3)$$

where \mathcal{D} is the scattering angle, σ_c the bound coherent cross section, k_B is Boltzmann's constant, T the absolute temperature, M is the mass of the scattering atom, m the neutron mass and S_s, S_d are the "self" and "distinct" part of the scattering law.

The introduction of the relative units α and B , now often used, is in principle only advantageous for a perfect gas. In the more general case $S(\alpha, B)$ still depends in a complicate way on the temperature.

A number of practicable theoretical models have been proposed to describe $S(\vec{k}, \omega)$ or $S(\alpha, B)$. For example the scattering from isolated molecules neglecting the interaction between rotations and vibrations has been described in different approximations [1,2]. The scattering from ideal solids has been handled in the harmonic approximation taking multiphonon processes into account for incoherent scattering [3] and restricting so far to one-phonon processes in the coherent case [4].

For liquids the situation is even more unsatisfactory. Several proposals to describe the diffusive motions of the constitutive particles quantitatively have been made [5]. First attempts have been made to treat hindered rotation of molecules in liquids [6].

A large number of scattering law calculations for moderators start with the Gaussian approximation for the intermediate scattering function $I(\alpha, t)$ in the time-dependent formalism [7].

$$S_s(\alpha, \beta) = \frac{1}{2\pi} \int_{-\infty}^{+\infty} I(\alpha, t) e^{i\beta t} dt \quad (4)$$

where

$$I(\alpha, t) = \exp\left\{-\alpha \int \frac{\rho(\beta)}{\beta \sinh(\beta/2)} [\cosh \beta/2 - \cos \beta t] d\beta\right\} \quad (5)$$

$\rho(\beta)$ is a generalized frequency distribution which in the case of harmonic vibrating solids of cubic symmetry having one atom per unit cell is identical to the normalized density of lattice vibration modes. $\rho(\beta)$ can be derived from $S(\alpha, \beta)$ by extrapolating $S(\alpha, \beta)/\alpha$ to $\alpha = 0$.

$$\rho(\beta) = \frac{\beta}{2} \sinh \frac{\beta}{2} \left(\frac{S}{\alpha}\right)_{\alpha=0} \quad (6)$$

For more general systems $\rho(\beta)$ is not directly the density of the vibration modes, e.g. because of the influence of polarisation vectors in solids. But it still describes the spectral density of the motions of a single atom and can be defined quite generally as the Fourier transform of the imaginary part of the atom's velocity auto-correlation function [8]. Starting from $\rho(\beta)$, $S_s(\alpha, \beta)$ can be completely reconstructed.

There remains much more work to be done to get satisfactory models for the different systems of condensed matter.

It should be stressed however, that in the field we are interested here, the thermalization of neutrons in reactors, the integral quantities to be calculated often do not depend strongly on the details of the scattering law. Dependent from the point of view this may be an advantage or disadvantage. Calculations even with crude models often give sufficient accurate results for these integral quantities of practical interest. This fact on the other hand makes it difficult to use, e.g., measured thermalization properties as a check for the validity of models or the accuracy of measured scattering laws. This is a point to which we will come back later on.

There are certain well understood general properties of $S(\vec{\kappa}, \omega)$, which to observe is more important for neutron thermalization than the realistic description of details. These properties are expressed by the following relations.

a) Principle of detailed balance

$$S(-\vec{\kappa}, -\omega) = e^{-\frac{\hbar\omega}{k_B T}} S(\vec{\kappa}, \omega) \quad (7)$$

This is a consequence of the microscopic reversibility of scattering processes. Although Eq. (7) is no necessary condition, it guarantees that the solution of the Boltzmann equation for a nonabsorbing infinite medium is a Maxwellian distribution.

By extracting the factor $\exp(-\beta/2)$ and introducing the function $S(\alpha, \beta)$, a symmetrical function in β , in Eq. (3) the relation (7) is always fulfilled.

b) Moment relations

The first few of these moment theorems originally derived by Placzek [9] are

$$\int S_s(\vec{\kappa}, \omega) d\omega = 1, \quad \int S_c(\vec{\kappa}, \omega) d\omega = 1 + \chi(\vec{\kappa}) \quad (8)$$

$$\int S(\vec{\kappa}, \omega) \omega d\omega = \frac{\kappa^2}{2M} \quad (9)$$

$$\int S(\vec{\kappa}, \omega) \omega^2 d\omega = \frac{\kappa^2}{M} k_B T \quad (10)$$

where $\chi(\vec{\kappa})$ is the Fourier transform of the static pair-distribution in the coherent case. Eq. (9) is well known as the "sum rule", which says that for any system of chemical bound atoms the average energy transfer $\overline{\hbar\omega}$ for a momentum transfer $\hbar\kappa$ is the same as if the atoms were free.

Eq. (8), (9) and (10) guarantee the high energy total scattering cross section to be the free atom cross section and should not be violated.

In these equations only measurable quantities appear, allowing us to use them as a check for experimental results.

II. Integral Properties of $S(\alpha, \beta)$

If the scattering law $S(\alpha, \beta)$ is complete (covering the whole α, β -range) and accurate enough, all physical properties influenced by the chemical binding of the atoms can be calculated.

Here we are mainly interested in integral properties describing aspects of neutron thermalization which can be evaluated from $S(\alpha, \beta)$ and determined or derived more directly from measurements on the other hand. Among these quantities are the total scattering cross section $\sigma(E_0)$, the average cosine of the scattering angle $\bar{\mu}(E_0)$, the differential scattering cross section $\sigma(E_0, \vartheta)$, the transport mean free path $\lambda_{tr}(E_0)$, the thermal diffusion constant D_0 , the second moment of energy transfer M_2 for a Maxwellian distribution and others.

A method quite common in use now for such calculations is to start from the generalized frequency distribution $\rho(\beta)$. $\rho(\beta)$ can be either measured directly using cold neutrons, derived from $S(\alpha, \beta)$ or constructed from other experimental data on the dynamics of the scatterer, e.g. from interatomic force constants, available from dispersion curve measurements. If the incoherent approximation is valid, the phonon expansion [3] and the short-collision-time approximation [10] are sufficient to calculate $S(\alpha, \beta)$ for the whole α - and β -range of interest. Several computer programmes to do these calculations, are now available, e.g. LEAP [11], SUMMIT [12], GAKER [13], UPRAS [14] and others.

Similarly programmes are in use for, calculating P_n -scattering matrixes, starting from $S(\alpha, \beta)$, e.g. PIXSE [15]. These are then used for the calculation of thermal spectra, for the numerical solution of transport problems and related topics.

Starting with the LEAP output, KAPIXSE [16], e.g., evaluates the coefficients of the expansion of $\sigma(E_0 \rightarrow E, \vartheta)$ in Legendre polynoms $P_1(\mu)$ ($\mu = \cos \vartheta$):

$$\sigma_1(E_0 \rightarrow E) = \frac{2}{2l+1} \int_{-1}^{+1} P_1(\mu) \sigma(E_0 \rightarrow E, \mu) d\mu \quad (11)$$

and further

$$\sigma(E_0) = \int dE \sigma_0(E_0 \rightarrow E), \quad \bar{\mu}(E_0) = \int dE \sigma_1(E_0 \rightarrow E) / \sigma(E_0) \quad (12)$$

The thermal diffusion constant is defined as

$$D_0 = \frac{\int_0^{\infty} M(E) \lambda_{tr}(E) dE}{3 \int_0^{\infty} M(E) dE} \quad (13)$$

where $M(E) = (k_B T)^{-2} E \exp(-E/k_B T)$ is the Maxwell distribution.

Another important parameter is M_2 , the second moment of energy transfer for a Maxwellian velocity distribution of the neutrons:

$$M_2 = (k_B T)^{-2} \int_0^{\infty} dE_0 \int_0^{\infty} dE M(E) (E - E_0)^2 \sigma(E \rightarrow E_0) \quad (14)$$

Within the Gaussian approximation for the scattering law, M_2 can be written [17]

$$M_2 = (15/16)(\sigma_b m/M) \int_{-\infty}^{+\infty} t \dot{w}(t) \sqrt{0.25 + t^2 + mw(t)/M}^{-7/2} dt \quad (15)$$

where

$$w(t) = \int_0^{\infty} \left[\frac{\rho(B)}{B \sinh(B/2)} \right] \left[\frac{\cosh(B/2) - \cos(Bt)}{2} \right] dB \quad (16)$$

III. Present State of the Experimental Technique

1. Experimental arrangement, technique of measurement

For the measurement of double differential cross sections a double spectrometer is necessary. This is an apparatus consisting of a primary spectrometer, a monochromator selecting from a thermal neutron source spectrum a beam with a small energy band of neutrons, and a secondary spectrometer for analyzing the energy and momentum of scattered neutrons.

Most of the scattering laws for materials we are interested in here are measured with the time-of-flight technique, using a pulsed monochromatic neutron beam and determining the energy after scattering by the time-of-flight of the neutrons.

As sources mainly thermal reactors with high fluxes have been used, also a number of experiments have been performed at linear accelerators.

The time-of-flight spectrometers in principle do not differ in the secondary part of the arrangement. The difference is mainly in the

primary part, the producing of the pulsed monochromatic beam. Because most of you are more familiar with the phased rotor systems used at Harwell and Chalk River [18], at the MTR (Idaho) [19], and here in Ann Arbor [20], I would like to show you the principle of a rotating crystal time-of-flight spectrometer which in the last few years has become a strong competitor to the mechanical chopper systems. Fig. 1 shows a scheme of the rotating crystal spectrometer in operation at the reactor FR 2 in Karlsruhe [21]. There are perhaps only two comments to be made:

- a) The rotating crystal is a relative simple technical device compared with a phased chopper and it has the advantage of offering several monochromatic beams simultaneously.
- b) Considering intensity and resolution crystal and double chopper are about equivalent. If the rotating crystal is optimized it is even superior to the chopper.

The present apparatus has a primary energy resolution of 2-5%. So far it was used for incident energies between 8 and 100 meV. Fig. 2 shows the part of the (κ, ω) -plane covered with this instrument and the range one probably would like to cover.

2. Data accumulation and reduction

Normally the large amount of data collected in such an experiment is stored in a multichannel analyzer, sequentially written on magnetic tape or, as we are doing it now, handled with an on-line computer having large capacity storage media like tapes and magnetic discs available. The totalized information for sample-in and-out runs normally available on a tape is converted in $S(\alpha, \beta)$ -values on a larger-computer. This data can be further condensed if the assumptions of a model like the generalized frequency distribution are valid or at least a good approximation. In this case the way to interpolate and extrapolate the data is obvious.

3. Multiple scattering

But often the " $S(\alpha, \beta)$ -values" derived in this way are not the quantities one really wishes to determine. Even with targets of transmission as high as 0.9 multiple scattering processes (neutron scattered twice or more often) contribute substantially to the measured cross section $\sigma(E_0 \rightarrow E, \theta)$. The correction for these contributions is in general,

especially for coherent scattering, a very complicate process. The searched quantity $S(\alpha, \beta)$ has to be known for the correction.

The approach we decided to make is to calculate this correction in incoherent approximation. Space-, angle- and energy dependent neutron currents $p_n(x, \mathcal{S}, E)$ are defined in the probe. Up to three collisions taking into account all possible combinations of elastic and inelastic processes are considered.

An iterative procedure was developed which starts by describing the experimentally determined $S(\alpha, \beta)$ -values by a phonon expansion (using a programm like LEAP [11], e.g.). The currents $p_n(x, \mathcal{S}, E)$ are then calculated. By comparing $p_1(x, \mathcal{S}, E)$, the quantity we are really interested in, with $S(\alpha, \beta)$ derived from the measurement a correction is found which leads to a new choice for the frequency distribution of the phonon expansion.

A computer programme (VIPER) has been written to do these evaluations [22]. In practice it was found that one or two iterations are sufficient to get the multiple scattering correction. Fortunately one finds often already for p_2 the typical angular dependence of the elastic scattering, thus allowing an estimation of higher p_n -terms and saving the large computer time necessary for $p_3(x, \mathcal{S}, E)$. A typical result of such a procedure is shown in Fig. 3.

Dependent upon α it was found that inelastic multiple scattering processes contribute substantially to the correction.

Similar calculations, restricted sometimes on elastic contributions however, have been done by others [23 - 25].

4. Resolution correction

Not much work has been done so far for correcting $S(\alpha, \beta)$ for the resolution of the spectrometer. A simple correction for lines unfolds two Gaussian distributions, giving again a Gaussian [26]. A more general procedure has been described by Maiorov et al. [27].

$S(\alpha, \beta)$ is calculated by direct time integration of the intermediate scattering function, introducing a Gaussian cut-off factor $\exp(-\sigma^2 t^2/2)$. The result is a convolution of the true scattering distribution with a Gaussian of width σ and this is just the quantity measured.

IV. Other Sources of Information

As we have seen, the present scattering law measurements with neutrons do not cover the whole part of interest of the (κ, ω) -plane and often the energy resolution is not sufficient enough to measure excitation energies accurate enough. Therefore results of other experimental techniques have to be taken into consideration, especially for the more complicated molecular liquids and solids, in the construction of a complete scattering law. For instance the frequencies of intramolecular vibrations are largely available from infra-red and Raman measurements and can be used to complete $\rho(\beta)$.

For simple single crystals phonon dispersion relation in a few symmetry directions or planes can be measured with an accuracy of a few percent using coherent neutron scattering or X-ray scattering. These measured dispersion curves are normally fitted with a several neighbors Born-von Kármán model to determine interatomic force constants. Techniques have been developed to calculate from these force constants the density of lattice vibration modes. Probably the most accurate method is at present the root sampling technique [28]. Because of the higher accuracy attainable in dispersion measurements, a frequency distribution derived in this way seems to be more reliable than one derived from a measured $S(\alpha, \beta)$ using the incoherent approximation and the extrapolation procedure of Eq. (6). The $\rho(\beta)$ calculated by the root sampling technique for an irreducible part of the Brillouin zone can then be used as input information for the Gaussian approximation.

It should be kept in mind, however, that for more complicate crystals what is needed is the spectral density of atomic motions rather than of normal modes. This essentially means that not $\rho(\beta)$ but $S(\alpha, \beta)$ has to be calculated with the root sampling technique.

Finally it should be mentioned that sometimes specific heat measurements allow the reconstruction of part of the frequency distribution or the determination of open parameters in a model assumption for $\rho(\beta)$ [29].

V. Discussion of Measured Scattering Laws

It is impossible to cover in a review like the present all the scattering law data measured so far. Therefore only a few important materials like water, zirconium hydride and graphite are selected. Other materials like

organics will be covered by other papers in this session, also the few results mentioned will be supplemented by further contributions.

1. Light water

a) Free H₂O molecules

Although the knowledge of the scattering properties of gaseous H₂O may be not of vital interest for direct reactor use, an experimental determination of $S(\alpha, \beta)$ may be a sensitive check of current theoretical models describing scattering from free molecules. Results of an experiment at 540°K and a pressure of 20 at. are shown in Fig. 4 [30]. It can be seen that the Krieger-Nelkin model calculations using an effective mass $\bar{M} = 1.9 M_H$ do not agree with the experiment. Obviously the differential cross section for scattering from a system of asymmetric tops has to be calculated in the H₂O case, which has been done so far only for low incident energies [31].

b) Liquid H₂O

A considerable amount of neutron scattering data has been collected for liquid H₂O. We restrict here on room temperature data, newer results for higher temperatures are also reported at this conference. Examples of $S(\alpha, \beta)$ -values from different authors [32 - 36] are shown in Fig. 5. The plot leads to an estimation of the consistency of the order of about 20% for most of the α, β -range covered.

Because of the mainly incoherent scattering of hydrogen the extrapolation technique leading to a generalized frequency distribution $\rho(\beta)$ may be a good model in this case if the harmonic approximation is still useful and if the influence of the difference in vibration amplitudes of H and O can be handled.

$\rho(\beta)$ was derived from the $S(\alpha, \beta)$ data shown above and further from several up-scattering experiments [37, 38] with cold neutrons, which have been converted directly to a frequency distribution on the basis of the same assumptions. A comparison of all these distributions is made in Fig. 6. The area of all curves is normalized to 0.5. Compared to the present attainable accuracy for such frequency distribution measurements for simpler systems like vanadium the agreement is quite satisfactory. The cold neutron data have the advantage of better resolution, especially at low β values, but it is difficult to correct

them for multi-phonon processes. The energy range covered by this distribution is generally divided in 3 regions:

- 1) Diffusive motions of molecules corresponding to small energy transfers. This effect does not show up in the given $\rho(\beta)$, it contributes also only a small part to the spectral density.
- 2) The β -range up to $\beta=1$ with bumps at about 8 meV and 22 meV is determined by vibrations of the whole molecules.
- 3) The region above $\beta=1$ is thought to be mainly related to librational motions (hindered rotations) of the molecules.

1) to 3) are approximated in the Nelkin model [39] by two δ -functions. The relative weights of these δ -functions at $\beta=0$ and $\beta=2,4$ are indicated in Fig. 6 by the height of the lines.

For the internal vibrations of the H_2O molecules which are assumed to be not much disturbed by liquid effects, energy levels at 0.205 eV, 0.428 eV and 0.450 eV have been derived from infra-red data. Only recently an indication of the binding mode at 0.205 eV was found in neutron scattering data [40]. The total weight of these levels in the spectral density should be about 0.5 because half of the six degrees of freedom of each pair of H-atoms in the molecule has to be assigned to vibrations and half to the low energy motions. This is essentially confirmed by the experimental results for the low energy part of $\rho(\beta)$ and was used for normalizing the curves of Fig. 6.

Although the Nelkin model was a major step from a free gas approximation to a realistic scattering kernel for H_2O , discrepancies remained between measured and calculated integral quantities. In fact this is not surprising if the low energy part of $\rho(\beta)$ which shows a considerable structure is just approximated by two δ -functions. Part of this discrepancy has been removed by allowing for the spatial anisotropy of the internal H_2O vibrations [41].

An other extension of the Nelkin model recently proposed by McMurry and Russell [36] treats water as a mixture of free molecules and of aggregates of molecules of two sizes. Amplitudes of a set of vibrational energies below 0.125 eV have been selected to fit the MTR scattering law data for room temperature H_2O . Although the general features of this model are reasonable the selected amplitudes may depend from the large multiple scattering contributions at small α .

Integral data for H₂O

We discuss now a few typical results evaluated from $S(\alpha, \beta)$ data for H₂O in comparison with measured quantities.

Fig. 7 shows a comparison of experimental $\sigma(E_0)$ data for H₂O at room temperature [42, 43] with different model calculations. The dotted curve is calculated with the Nelkin model, the anisotropic model gives the dashed line and the solid line is a KAPIXSE calculation using $\rho(\beta)$ given by Haywood [44]. The general agreement of the various results is quite good, however, this indicates only that $\sigma(E_0)$ is not very sensitive to the details of $S(\alpha, \beta)$.

The agreement between the various models is quite satisfactory again for M_2 given in table 1.

Table 1 Second moment of energy transfer M_2 for H₂O

| Model | M_2 (barns) | |
|---------|---------------|--------------------------|
| Nelkin | 49.05 | Honeck [45] |
| Nelkin | 47.9 | Kiefhaber [46] |
| Haywood | 46.5 | Gläser and Beckurts [47] |

The differences are showing up more pronounced in the differential cross section $\sigma(E_0, S)$ and in the average cosine $\bar{u}(E_0)$. Experimental results [48, 49] and model calculations for both are given in Fig. 8 and Fig. 9. The discrepancy can be partially reduced with the anisotropic vibration model for water [41] but it seems that the experimentally determined scattering kernel yields the best agreement with the measured \bar{u} values. Because \bar{u} determines important quantities for reactor applications like the transport mean free path λ_{tr} and the thermal diffusion constant D_0 , the experimental determined scattering data should be taken into account in the construction of a final scattering kernel.

An other check of the data is possible with diffusion parameters derived from pulsed neutron measurements. Here the time constant α of the decay of an asymptotic spectrum is correlated with the geometrical buckling B^2 of the moderator assembly by a series of the type

$$\alpha = \frac{1}{v} \bar{\Sigma}_a + D_0 B^2 - CB^4 + FB^6 + \dots \quad (17)$$

Table 2 gives more recent results for the parameters.

Table 2 Diffusion parameters in H₂O at 20°C

| D_0 (cm ² sec ⁻¹) | C (cm ⁴ sec ⁻¹) | F (cm ⁶ sec ⁻¹) | |
|--|--|--|------------------------------|
| 35630 ± 80 | 3420 ± 170 | 214 ± 139 | experimental [50] |
| 37045 | 3361 | 169 | Nelkin kernel [51] |
| 34520 | 4220 | 363 | Haywood $\rho(\beta)$ [44] |

Influence of the scattering law on thermal neutron spectra

Neutron spectra measurements also offer the possibility to compare the various scattering models with experimental data. The type of experiment to be done depends on the property of the scattering model to be checked. If the energy transfer $\Sigma(E_0 \rightarrow E)$ is of interest only, spectra from large (poisoned) homogeneous systems which are not sensitive to the angular dependence of the scattering kernel can be measured. Spectra from the boundaries of moderators, however, depend in principle on the energy transfer and angular dependent properties of $S(\alpha, \beta)$. The possibilities of time-dependent spectra measurements, which may be more sensitive to the details of the scattering model, are not fully exploited yet.

Experiments of various types have been reviewed elsewhere [44, 52] and will be discussed at this symposium. A typical example of the first type is given in Fig. 10, where a spectrum from boron-poisoned H₂O measured by Poole [44] is compared with calculations using the Nelkin model and the frequency distribution $\rho(\beta)$ derived by Haywood. Although the Nelkin kernel is a considerable improvement over the free gas kernel, here, similarly as in the comparison for integral parameters we did above, a final discrepancy still exists which is reduced further by experimental scattering law data.

2. Zirconium hydride

In the ZrH_x lattice the H-atoms are placed in the center of a tetraeder formed by the heavy Zr atoms. Because of the high bound hydrogen cross section, neutrons see in first approximation a system of isotropic harmonic oscillators. Then from a theoretical point of view zirconium hydride or more general the metal hydrides are perhaps the simplest of

all moderators. The oscillator frequency $\hbar\omega$ has been experimentally determined by several workers to be about 0.14 eV. Up to four excited levels have been found with no substantial change in $\hbar\omega$. Further a line width $\Delta\hbar\omega$ of about 30 meV was determined for the first level without a detectable angular and temperature dependence. Results for $\hbar\omega$ and $\Delta\hbar\omega$ of the first level are summarized in table 3.

Table 3 Energy and linewidth of the optical level in zirconium hydride

| composition | ZrH _{0.5} | ZrH _{1.08} | ZrH _{1.5} | ZrH _{1.5} | — | ZrH ₂ | ZrH ₂ | ZrH ₂ |
|---------------------------|--------------------|---------------------|--------------------|--------------------|-----|------------------|------------------|------------------|
| T(°C) | 27 | 210 | 20 | 393 | 23 | 27 | 20 | 20 |
| $\hbar\omega$ (meV) | 140-145 | 138 | 130 | 130±5 | 136 | 140-145 | 137 | 140 |
| $\Delta\hbar\omega$ (meV) | 28 | 36 | 29.5 | 31 | 28 | 28 | 29 | 26.4 |
| reference | 53 | 54 | 55 | 56 | 57 | 53 | 58 | 59 |

By assuming a Debye-spectrum with a cut-off at 20 meV for the acoustical modes of the zirconium lattice and the line discussed above for the spectral density of optical modes a reasonably accurate scattering kernel has been constructed by Young *et al.* [60]. The weight to be assumed for the acoustical modes, although it is small, is somewhat arbitrary in this model. An attempt to determine this part of the frequency distribution from the specific heat was made by Reichardt [29]. He arrived at a cut-off energy of 27 meV. A direct determination of $\rho(\beta)$ from measured scattering law values for ZrH_{1.08} at T = 210°C using the extrapolation technique has been made recently by Ehret [54]. The result of this measurement is compared with the constructed $\rho(\beta)$ s in Fig. 11. The area of the measured acoustical part, corresponding also approximately to a Debye spectrum with a cut-off at 27 meV, is about 0.006. From general arguments it follows that this area of $\rho(\beta)$ depends on the hydrogen concentration in ZrH_x. The experimentally determined total area of $\rho(\beta)$ is about 20% lower than the theoretical value 1. This deviation is thought to be caused by the Zr atoms which have to be taken into account in principle with a different $\rho(\beta)$.

Integral properties for zirconium hydride

For the synthetical $\rho(\beta)$ models and the experimentally determined $\rho(\beta)$ various calculations of $\sigma(E_0)$, $\sigma(E_0, \beta)$ and $\bar{u}(E_0)$ have been made in the incoherent approximation. Results for $\sigma(E_0)$ at room temperature are

compared with the experimental data in Fig. 12. Besides the coherent contribution of Zr to $\sigma(E_0)$ above 4 meV the agreement is better than a few percent.

Experimentally determined $\sigma(E_0, \theta)$ values by Kornbichler [61] show a considerable structure, probably due to coherent Zr scattering, and therefore can be described only on the average by the models given above. The degree of agreement is demonstrated in Fig. 13. Similar measurements have been made by Beyster et al. [49]. In the average cosine $\bar{u}(E_0)$ (Fig. 14) the coherent effects are smoothed out again. There is however a sudden change of \bar{u} at the energy of the Einstein oscillator which is also reasonably well described by the models.

3. Graphite

Several experiments have been performed to measure the scattering of thermal neutrons from graphite at different temperatures [62 - 64]. The results of a more recent series of measurements by Carvalho [65] on different types of graphite at a temperature of 533°K are given in Fig. 15. Incident neutron energies E_0 have been between 17.5 and 95.5 meV. Plotted is again the symmetrical form of the scattering law $S(\alpha, \beta)$. Because data for different E_0 and for positive and negative β have to be on the same curve this representation gives an impression of the experimental accuracy. The curves show a considerable amount of structure which is marked at low β and low α and tends to wash out at larger α and higher β values. This structure which has not been so clear in the earlier experiments has its origin of course in the predominant coherent scattering of carbon. All data have been corrected for multiple scattering. The correction is serious for small α , reducing $S(\alpha, \beta)$ almost by a factor 5 for the lowest α values measured.

To explain the details of the experimental results, the coherent scattering law has to be calculated. On the other hand the simplest model one can try to compare with the measurement is a phonon expansion for the scattering law in the incoherent approximation. The result of such a calculation with a generalized frequency distribution derived from the experimental data in an iterative procedure is given by the dashed lines in Fig. 15. The corresponding frequency distribution is shown in Fig. 16 where it is compared with the distribution calculated with the root-sampling technique for the Yoshimori-Kitano model [66].

The latter one was adjusted to get agreement with the measured specific heat of reactor grade graphite. The demands on the extrapolated distribution should not be too high in view of all the approximations made. But it may be interesting that the specific heat of graphite can be described surprisingly well with this $\rho(\beta)$, which has no adapted parameters in it. Several other integral properties where directional effects are not very important can be reproduced with a similar accuracy.

Scattering law measurements for room temperature reactor grade graphite have been done recently by Whittemore [67] for higher energy and momentum transfers. These data, although they show less structure, can be well described with the frequency distribution derived above. Part of these data in comparison with calculations is shown in Fig. 17.

The actual behaviour of $S(\alpha, \beta)$ and angular dependent phenomena described by $S(\alpha, \beta)$ cannot be understood in the incoherent approximation.

Takahashi [68] made a detailed theoretical study of the coherent one-phonon cross section of polycrystalline graphite starting with the lattice model of Yoshimori and Kitano [69]. Besides the frequencies the polarization vectors of the phonons are needed for the calculation of the coherent scattering. $S(\alpha, \beta)$ has been separately calculated for in-plane and out of plane modes by sampling 675 values of the wave vector in an irreducible part of the first Brillouin zone. A typical result for one β value is shown in Fig. 18. In the same Fig. experimental data of Egelstaff [62] and temperature converted data of Carvalho are shown. Unfortunately this conversion is not allowed strictly because of multi-phonon contributions making the comparison somewhat arbitrary. However at least an overall agreement between experiment and calculation can be seen. The difference between the two experimental set of points at small α may be largely due to multiple scattering.

Integral data for graphite

To the authors' knowledge no calculations of integral scattering properties of graphite have been done so far taking coherent scattering into account. A lot of calculations have been done in the incoherent approximation either with the extrapolated $\rho(\beta)$ distributions or the frequency density derived from the Yoshimori-Kitano model. Here even the total cross section because of its coherent structure cannot be used as a reasonable check. All model calculations have in common that they yield below the

Bragg cut-off an inelastic contribution to $\sigma(E_0)$ which is about a factor two lower than the experimental points [42]. This discrepancy is not fully explained up to now.

The average cosine $\bar{\mu}(E_0)$ calculated for two $\rho(\beta)$ s is given in Fig. 19. No direct measurement of $\bar{\mu}$ (angular distribution type) has been done so far. Calculations of the second moment of energy transfer M_2 as a function of temperature are given in Fig. 20.

4. Other moderators

a) D_2O

Measurements of $S(\alpha, \beta)$ have been done by Haywood and Thorson [70] at $20^\circ C$ and $150^\circ C$. The generalized frequency distribution $\rho(\beta)$ for different temperatures was determined also from cold neutron measurements [71]. An adjustment of the Nelkin model parameters for the description of D_2O in the incoherent approximation has been given by Honeck [72] which was successful in describing total cross section and spectra. A careful study of coherent scattering was made by Butler [73]. He and Koppel and Young [74] showed that the interference effects tend to cancel.

b) Beryllium and beryllium oxide

The only experimental determinations of $S(\alpha, \beta)$ for polycrystalline material of these two moderators have been made by Sinclair [75]. He tried also to derive a generalized frequency distribution using the extrapolation technique. Young and Koppel [76] used the results of phonon dispersion measurements of Schmunk et al. [77] to calculate the frequency spectrum of beryllium with the sampling technique. There is a considerable difference between the calculated frequency distribution and the $\rho(\beta)$ extrapolated from $S(\alpha, \beta)$ measurements.

For beryllium oxide no theoretical calculation of the frequency distribution has been made so far. Such a calculation is more laborious than for Be because of the presence of two different atomic species in the lattice. On the other hand the use of the incoherent approximation for calculating $S(\alpha, \beta)$ is even more doubtful than for beryllium. It seems that for beryllium oxide further theoretical and experimental investigations are needed.

VI. Summary and Conclusions

In the last few years scattering kernels became available which take into account the influence of the different forms of chemical binding in matter on slow neutron scattering in a more realistic way than earlier. The experimental information used in constructing these kernels came from specific heat measurements, optical spectroscopy and inelastic neutron scattering experiments.

So far the scattering has been treated mainly in the incoherent approximation and the Gaussian approximation for the intermediate scattering function. Only in a few cases coherent scattering has been taken into account. For almost all the important moderators appropriate kernels are now available, which describe neutron thermalization in these materials in a satisfying way for many needs. A series of computer codes has been developed to make use of the available scattering law data to calculate scattering matrixes.

A few typical examples of available scattering law data have been discussed in this paper and it has been shown that inelastic neutron scattering experiments contributed considerably to our knowledge of neutron behaviour in matter in the energy range which is most important for neutron thermalization in reactors.

The experimental technique of scattering law measurements has reached a stage to deliver consistent results within an accuracy of $\pm 10\%$. This accuracy is good enough to reproduce the results of simpler but more precise integral measurements.

These measurements, mainly single differential cross section measurements, pulsed neutron experiments and to some extent spectra measurements, offer valuable checks for the various scattering law data generated.

The most sensitive check for synthetic kernels is to compare them with experimental scattering law data. But it seems that especially the differential cross section data are also quite sensitive to details of the scattering law. More systematic studies of this type are worthwhile.

Less work has been done so far on the temperature dependence of $S(\alpha, \beta)$. Also further experimental studies of the coherently scattering moderators are desirable. Probably the progress made in phonon dispersion work with neutrons will deliver a sound base for more accurate calculations for crystalline materials.

References

- [1] Krieger, T.J., and Nelkin, M.S., Phys. Rev. 106 (1957) 290.
- [2] Griffing, G.W., "Inelastic Scattering of Neutrons in Solids and Liquids" I, IAEA, Vienna (1963) 435.
- [3] Sjölander, A., Ark. Fys. 14 (1958) 315.
- [4] Iijima, S., J. Nucl. Sci. Technol. 3 (1966) 160.
- [5] Sjölander, A., in "Thermal Neutron Scattering", ed. by P.A. Egelstaff, Academic Press (1965) 291.
- [6] Yip, S. and Osborn, R.K., Phys. Rev. 130 (1963) 1860.
- [7] Egelstaff, P.A. and Schofield, P., Nuclear Sci. and Engng. 12 (1962) 260.
- [8] Rahman, A., Singwi, K.S. and Sjölander, A., Phys. Rev. 126 (1962) 986.
- [9] Placzek, G., Phys. Rev. 86 (1952) 377.
- [10] Wick, G.C., Phys. Rev. 94 (1954) 1228.
- [11] Mc Latchie, R. Program description LEAP, AERE Harwell (1962).
- [12] Bell, J., USAEC Report GA-2492 (1962).
- [13] Honeck, H.C., BNL-5826 (1961).
- [14] Maiorov, L.V., Turchin, V.F. and Yudkevich, M.S., Proc. 3rd UN Int. Conf. Vol. 2. (1965) 379.
- [15] MacDougall, J.D., AEEW-M 318 (1963).
- [16] Stittgen, H., Internal Report, Karlsruhe (1964).
- [17] Schofield, P. BNL 770 (T-288) (1962).
- [18] Egelstaff, P.A., Cocking, S.J. and Alexander, T.K., "Inelastic Scattering of Neutrons in Solids and Liquids", IAEA, Vienna (1961) 165.
- [19] Brugger, R.M. and Evans, J.E., Nucl. Instr. Methods 12 (1961) 75.
- [20] Zweifel, P.F., Report O3712-S-P, University of Michigan (1964).
- [21] Carvalho, F., Ehret, G., Gläser, W. and Ripfel, H., KFK 263 (1964).
- [22] Carvalho, F. and Ehret, G., Internal Report Karlsruhe (1966).
- [23] Honeck, H.C., GA-5968 (1964).
- [24] Cocking, S.J. and Heard C.R.T., AERE-R.5016 (1965).

- [25] Thorson, I.M., Priv. comm.
- [26] Greenspan, H. and Baksys, I.G., ANL Reactor Physics Constants Center, Newsletter No. 3 (1962).
- [27] Maiorov, L.V., Turchin, V.F. and Yudkevich, M.S., Proc. 3rd UN Int. Conf. Vol. 2. (1965) 379.
- [28] Gilat, G. and Raubenheimer, L.J., Phys. Rev. 144 (1966) 390.
- [29] Reichardt, W., this conference, paper SM 96/15.
- [30] Merkel, A., Internal report, Karlsruhe (1966).
- [31] Khubchandani, P.G. and Rahman, A., J. Nucl. Energy 11 (1960) 89.
- [32] Egelstaff, P.A., AERE-R 3931, Harwell (1962).
- [33] Kotwitz, D.A. and Leonard, J.R., "Inelastic Scattering of Neutrons in Solids and Liquids" I, IAEA Vienna (1963) 359.
- [34] Haywood, B.C., AERE-R 4484, Harwell (1964)
- [35] Mostovoy, V.I. et al. , Proc. 3rd UN Int. Conf. Vol.2 (1965) 280.
- [36] McMurry, H.C., Russell, G.J., Brugger, R.M., Nucl. Sci. Engng. 25 (1966) 248.
- [37] Larsson, K.E. and Dahlborg, U., React. Sci. Technol. 16 (1962) 81.
- [38] Blanckenhagen, P.v., Karlsruhe (unpublished).
- [39] Nelkin, M.S., Phys. Rev., 119 (1960) 741.
- [40] Harling, O.K., Phys. Letters 22 (1966) 15.
- [41] Koppel, J.U. and Young, J.A., Nucl. Sci. Engng. 19 (1964) 412.
- [42] BNL 325.
- [43] GA-4659 (1963) 25.
- [44] $\rho(\beta)$ given by Poole in Pulsed Neutron Research, Vol. I, IAEA Vienna (1965) 425.
- [45] Honeck, H.C., Nucl. Sci. Engng. 18 (1964) 49.
- [46] Kiefhaber, E., Private Comm.
- [47] Gläser, W. and Beckurts, K.H., Nucl. Sci. Engng. 20 (1964) 235.
- [48] Springer, T., Hofmeyr, C., Kornbichler, S. and Lemmel, H.D., Proc. 3rd UN Int. Conf. Vol. 2 (1965) 351.
- [49] Beyster, J.R., Young, J.C. Neill, J.M. and Mowry, W.R., Pulsed Neutron Research, Vol. I, IAEA Vienna (1965) 407.

- [50] Arai, E. and Kuchle, M., Nukleonik, 7 (1965) 416.
- [51] Ghatak, A.K. and Honeck, H.C., Nucl. Sci. Engng. 21 (1965) 227.
- [52] Beyster, J.R. and Neill, J.M., U.S.A.E.C. CONF-660303 (1966) 91.
- [53] Whittmore, W., GA 4490 (Rev.).
- [54] Ehret, G., Karlsruhe (unpublished) (1966).
- [55] Pelah, I., Eisenhauer, C.M., Hughes, D.J. and Palevsky, H., Phys. Rev. 108 (1957) 1091.
- [56] Andresen, A., Mc Reynolds, A.W., Nelkin, M., Rosenbluth, M. and Whittmore, W., Phys. Rev. 108 (1957) 1092.
- [57] Woods, A.D.B., Brockhouse, B.N., Sakamoto, M., Sinclair, R.N., "Inelastic Scattering of Neutrons in Solids and Liquids", IAEA Vienna (1961) 487.
- [58] Pan, S.S. and Webb, F.J., Nucl. Sci. Engng. 23 (1965) 188.
- [59] Harling, O.K., Rev. Sci. Instr. 37 (1966) 697.
- [60] Young, J.C., Young, J.A., Houghton, G.K., Trimble, G.D. and Beyster, J.R., Nucl. Sci. Engng. 19 (1964) 230.
- [61] Kornbichler, S., Nukleonik 7 (1965) 281.
- [62] Egelstaff, P.A. and S.J. Cocking, "Inelastic Scattering of Neutrons in Solids and Liquids", IAEA Vienna (1961) 25 and AERE-R 3931 (1962).
- [63] Dolling, G. and Brockhouse, B.N., Phys. Rev. 128 (1962) 1120.
- [64] Haywood, B.C. and Sinclair, R.N., AERE-R 4732 (1964).
- [65] Carvalho, F., Doctor thesis, Karlsruhe (1967).
- [66] Young, J.A. and Koppel, J.U., J. Chem. Phys. 42 (1965) 357.
- [67] Whittmore, W., Private comm.
- [68] Takahashi, H., Private comm.
- [69] Yoshimori, A. and Kitano, Y., J. Phys. Soc. Japan 11 (1956) 352.
- [70] Haywood, B.C. and Thorson, I.M., BNL 719 (C-32) (1962) 27.
- [71] Dahlborg, U., Gresshög, G., Larsson, K.E., Möller, E., Purohit, S.N. and Sjöstrand, N.G., Proc. 3rd UN Int. Conf. Vol. 2 (1965) 336.
- [72] Honeck, H.C., Trans. Am. Nucl. Soc. 5 (1962) 47.
- [73] Butler, D., Proc. Phys. Soc. 81 (1962) 276 and 294.

- [74] Koppel, J.U. and Young, J.A., Nukleonik 7 (1965) 408.
- [75] Sinclair, R.N., "Inelastic Scattering of Neutrons in Solids and Liquids" Vol. II, IAEA Vienna (1963).
- [76] Young, J.A. and Koppel, J.K., Phys. Rev. 134 (1964) 1476.
- [77] Schmunk, R.E., Brugger, R.M., Randolph, P.D. and Strong, K.A., Phys. Rev. 128 (1962) 562.

Caption of Figures

- Fig. 1 Rotating crystal time-of-flight spectrometer at the FR2.
- Fig. 2 Attainable κ, ω -range for different incident energies E_0 .
- Fig. 3 Examples of multiple scattering corrections.
- Fig. 4 Examples of $S(\alpha, \beta)$ for gaseous H_2O .
- Fig. 5 $S(\alpha, \beta)$ data for H_2O at $295^\circ K$ for two values of β .
- Fig. 6 Frequency distributions for room temperature H_2O .
- Fig. 7 Total cross section of H_2O .
- Fig. 8 $\sigma(E_0, \vartheta)$ of H_2O for an incident energy $E_0 = 44$ meV.
- Fig. 9 Average cosine $\bar{\mu}(E_0)$ for H_2O .
- Fig. 10 Calculated spectra in comparison with experimental data for boron-poisoned H_2O [44].
- Fig. 11 Frequency distributions of zirconium hydride.
- Fig. 12 Total cross section of zirconium hydride.
- Fig. 13 $\sigma(E_0, \vartheta)$ of zirconium hydride.
- Fig. 14 Average cosine $\bar{\mu}(E_0)$ of zirconium hydride.
- Fig. 15 Scattering law $S(\alpha, \beta)$ of graphite at $T=533^\circ K$.
- Fig. 16 Frequency distribution of graphite at room temperature.
- Fig. 17 $S(\alpha, \beta)$ for graphite at high α and β values.
- Fig. 18 Coherent one-phonon contribution to $S(\alpha, \beta)$.
- Fig. 19 Average cosine $\bar{\mu}(E_0)$ of graphite.
- Fig. 20 M_2 for graphite (free gas).

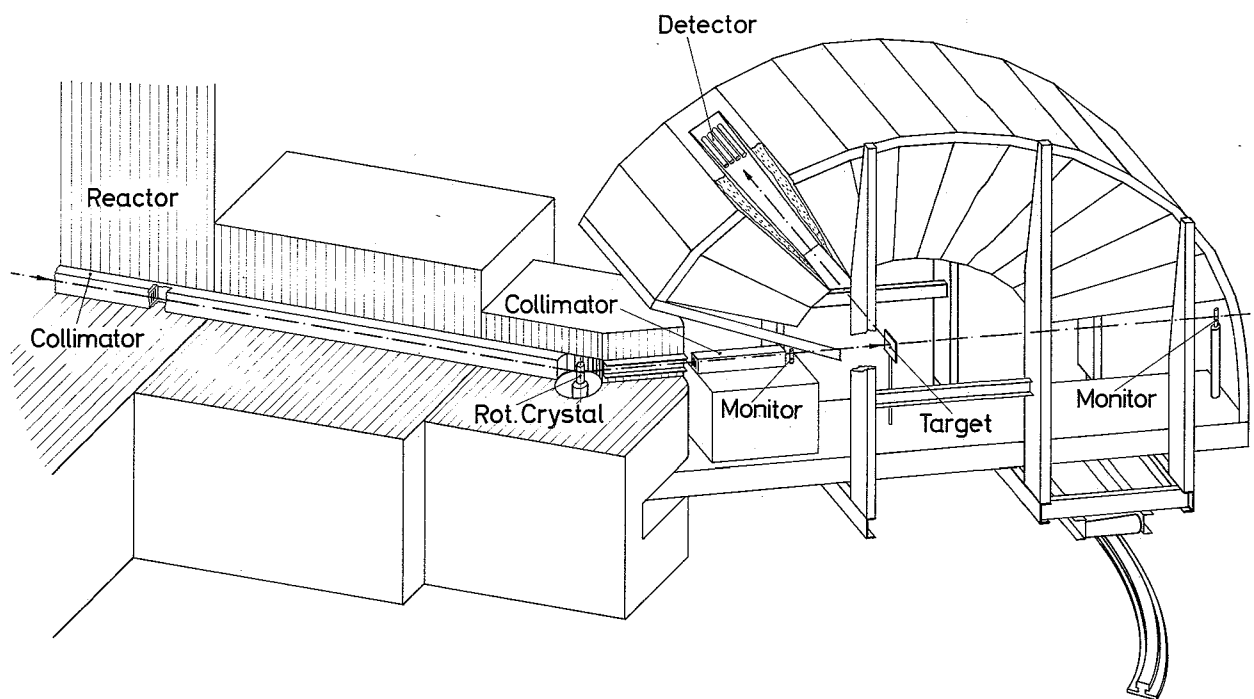


Fig.1 Rotating crystal time-of-flight spectrometer at the FR 2

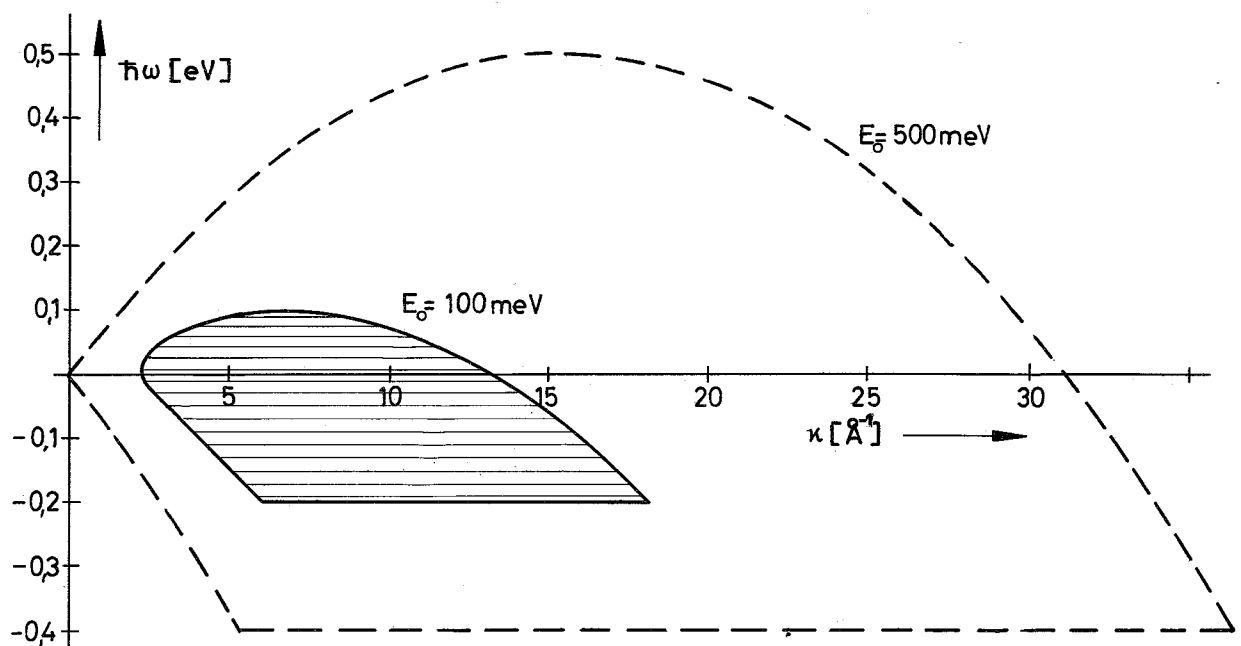


Fig. 2 Attainable κ, ω -range for different incident energies E_0

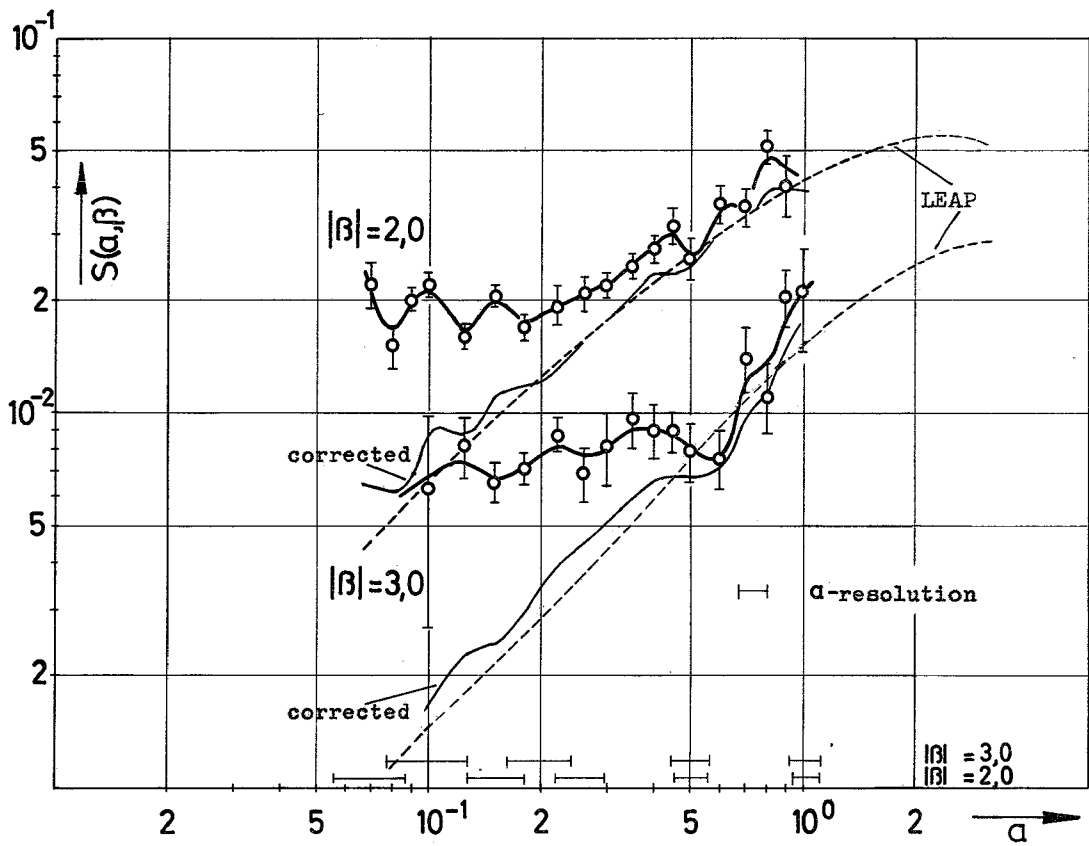


Fig. 3 Examples of multiple scattering corrections

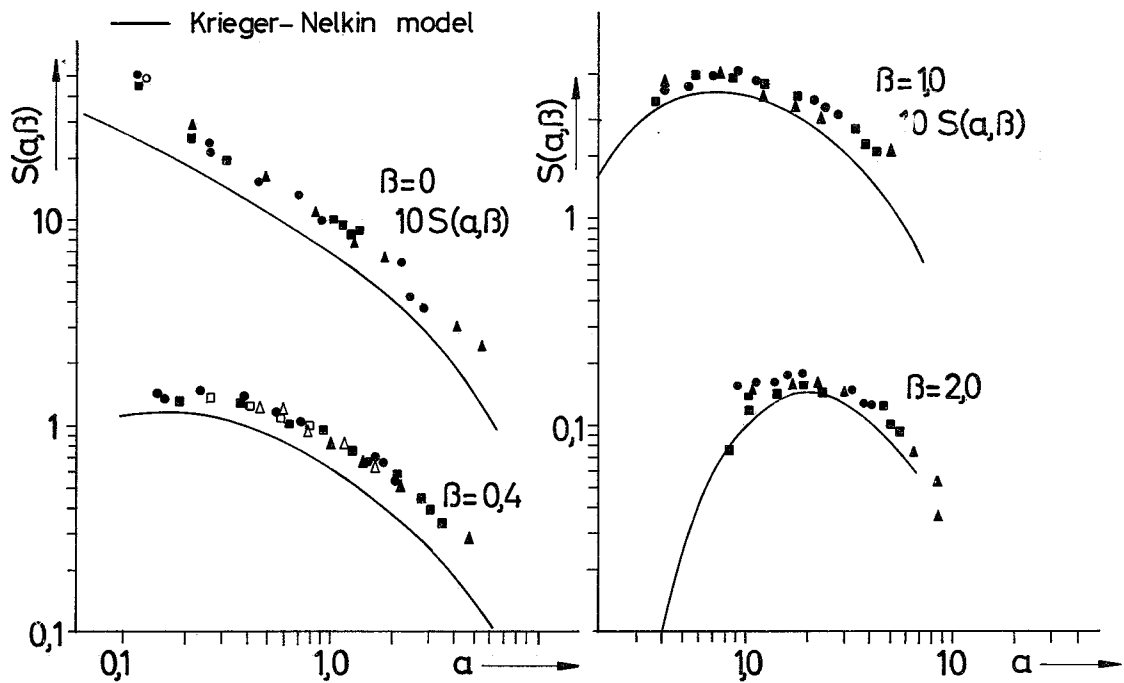


Fig.4 Examples of $S(a, \beta)$ for gaseous H_2O

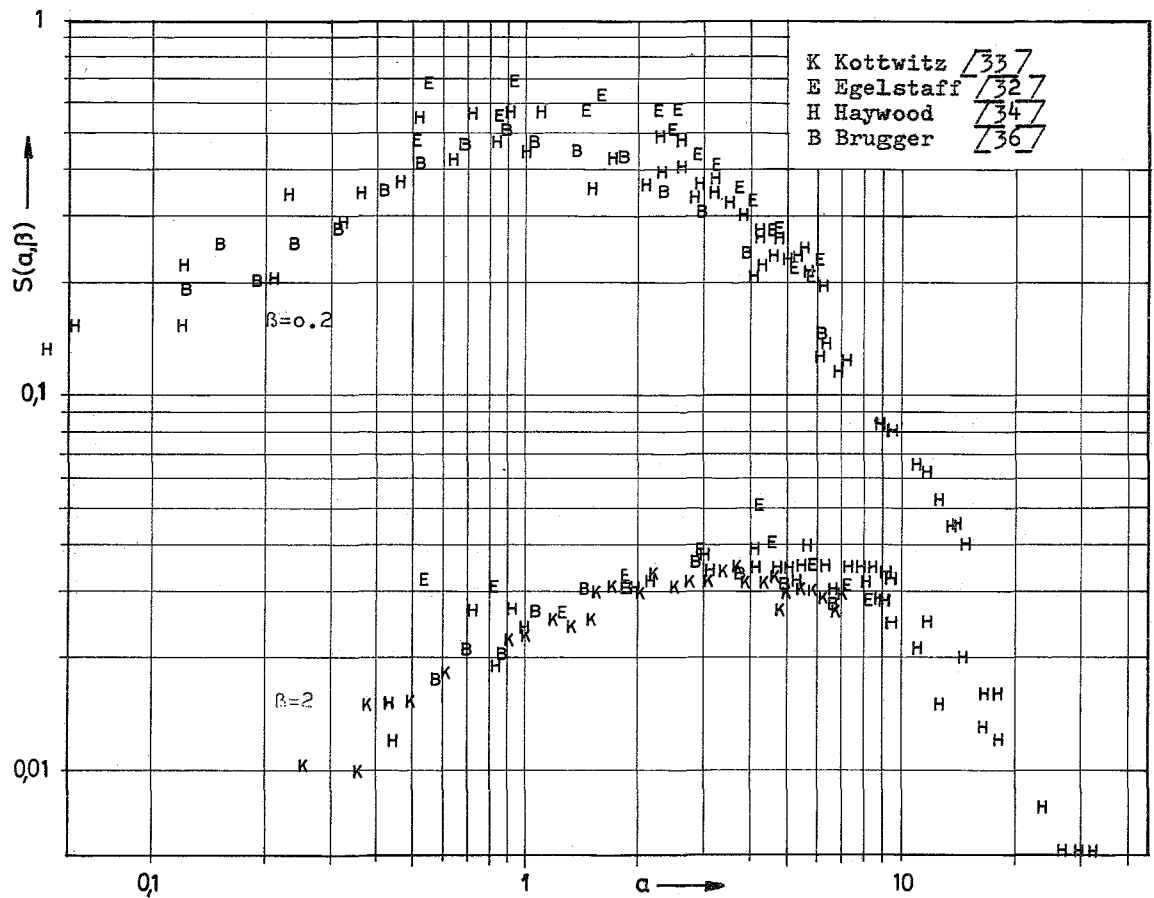


Fig. 5 $S(\alpha, \beta)$ data for H_2O at $295^\circ K$ for two values of β

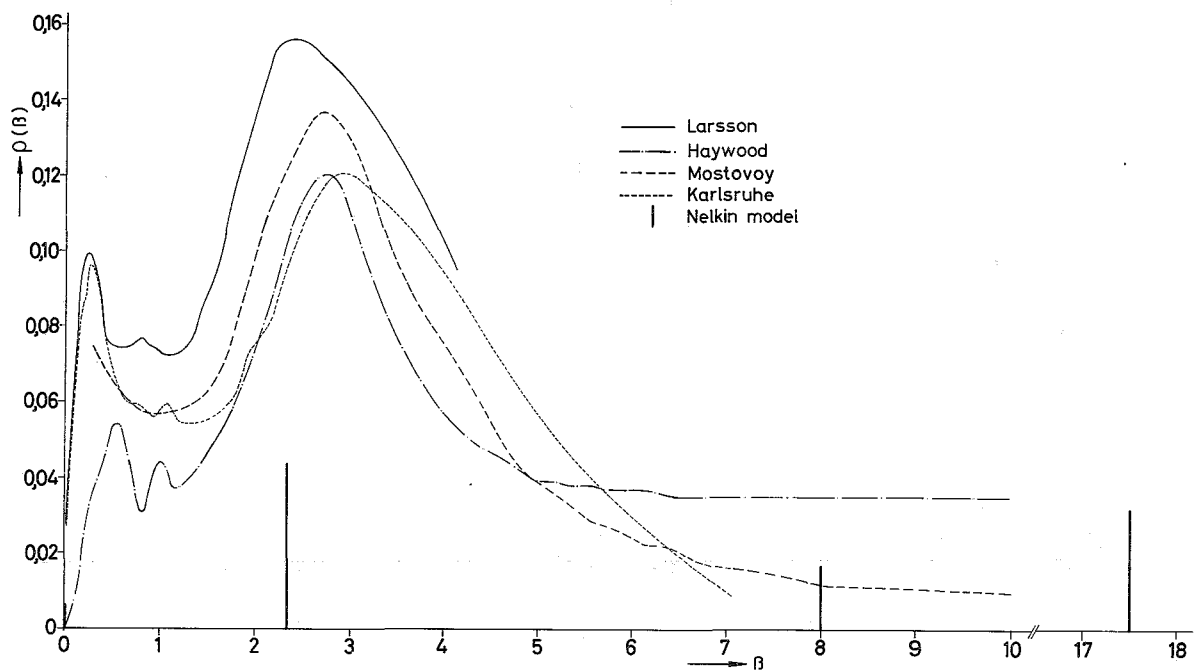


Fig. 6 Frequency distributions for room temperature H_2O

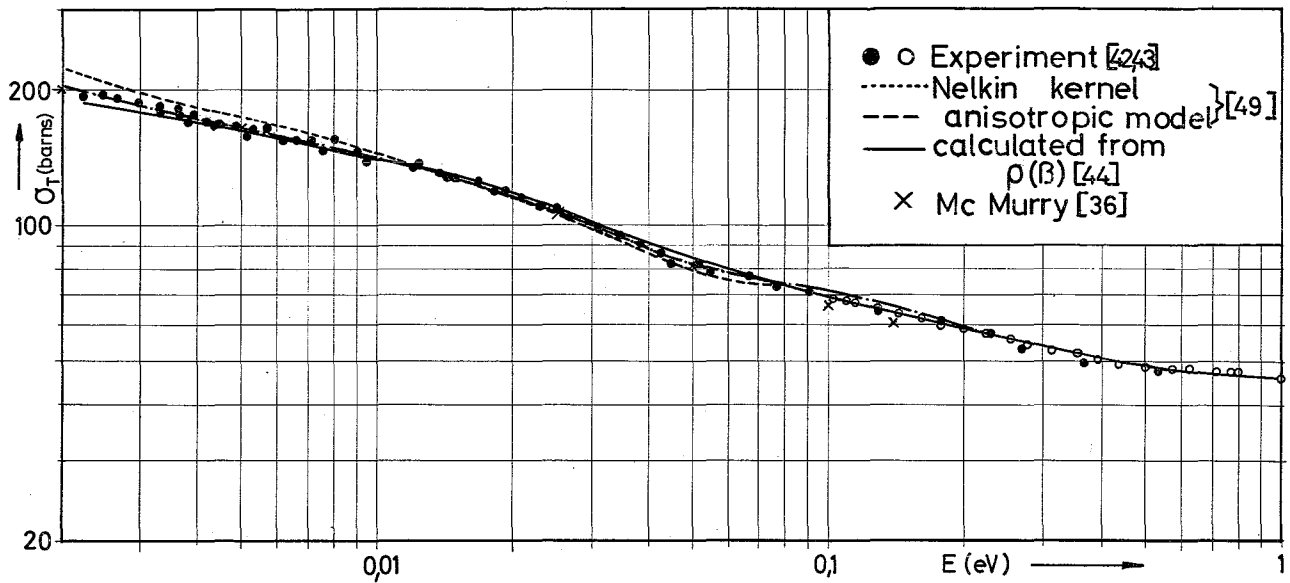


Fig.7 Total cross section of H₂O

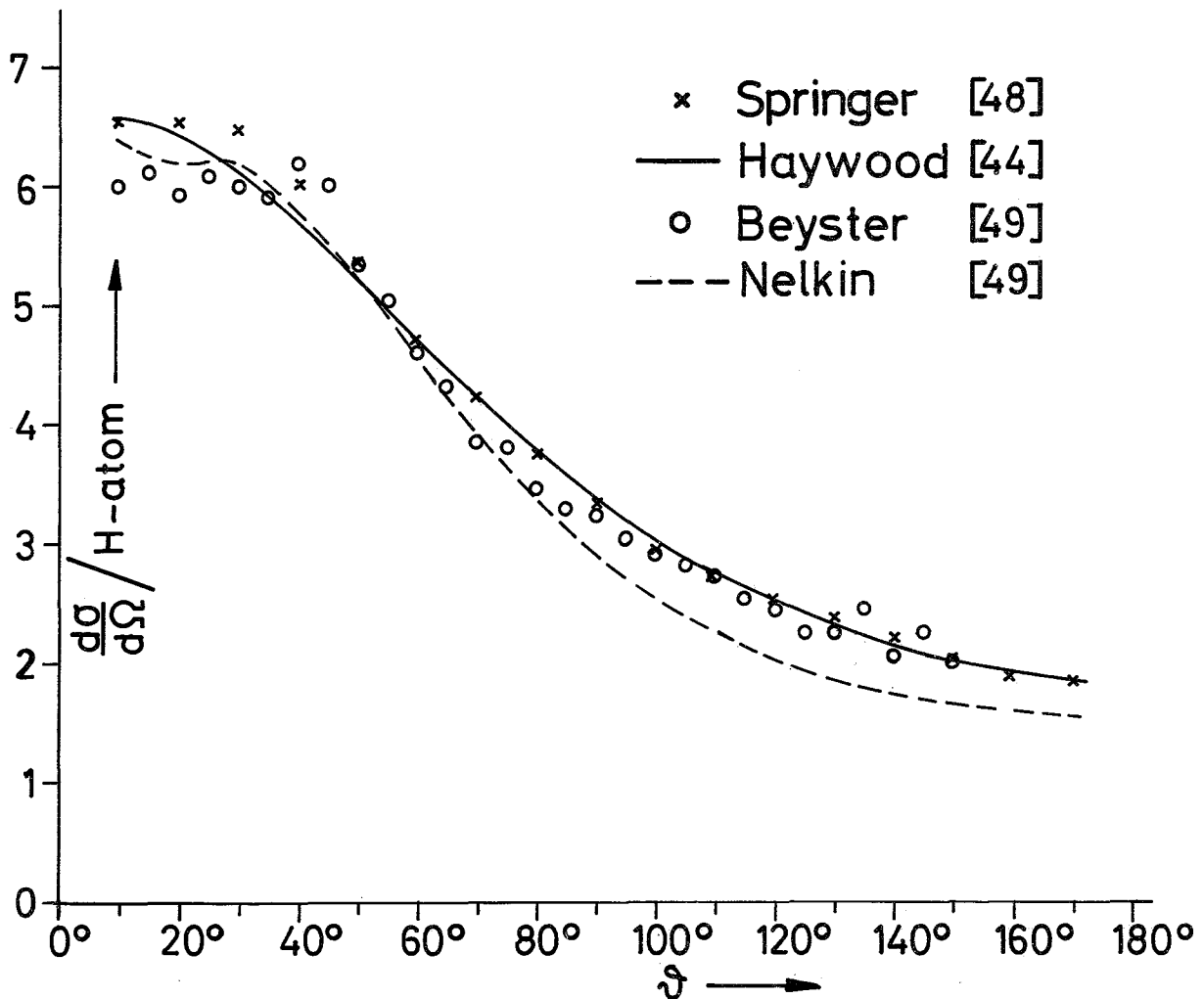


Fig.8 $\sigma(E_0, \vartheta)$ of H₂O for an incident energy $E_0=44\text{meV}$

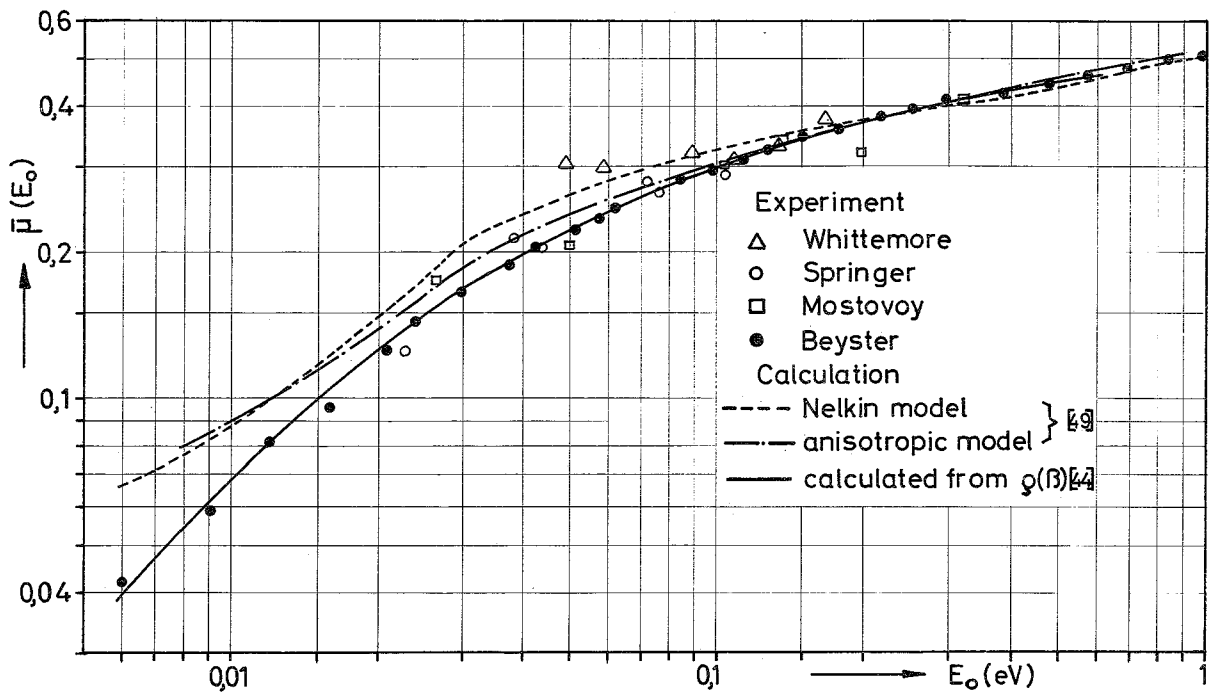


Fig.9 Average cosine $\bar{\mu}(E_0)$ for H_2O

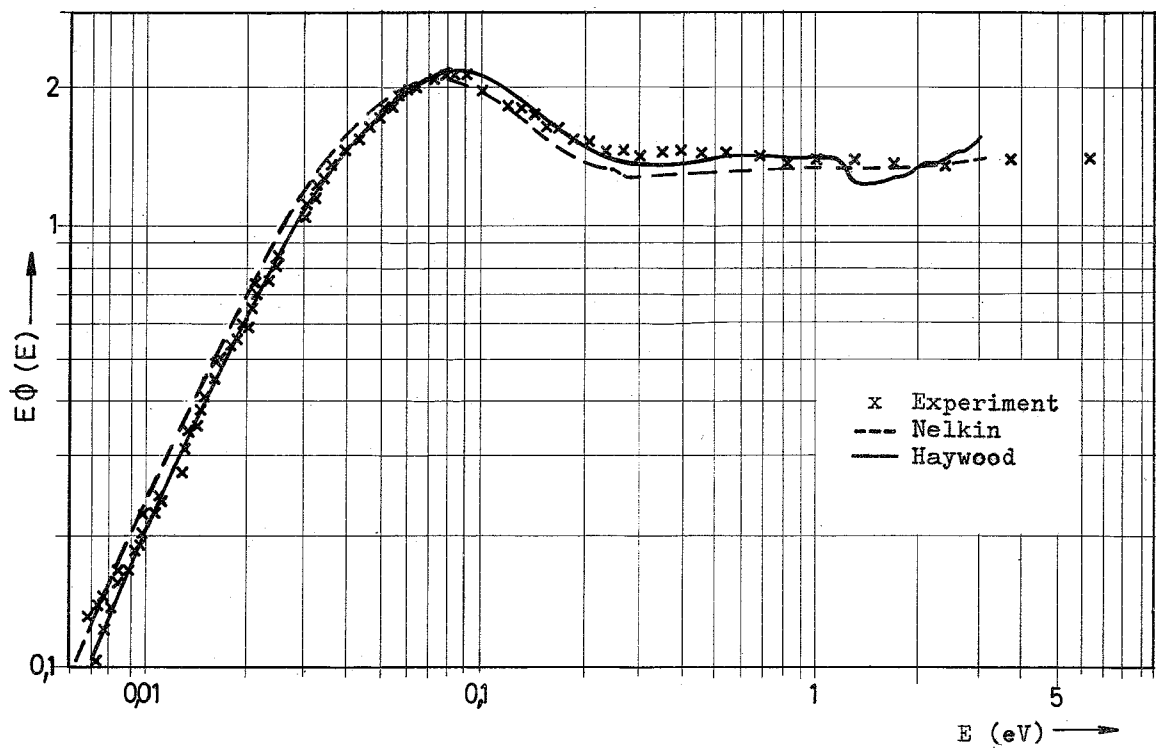


Fig. 10 Calculated spectra in comparison with experimental data for boron-poisoned H_2O

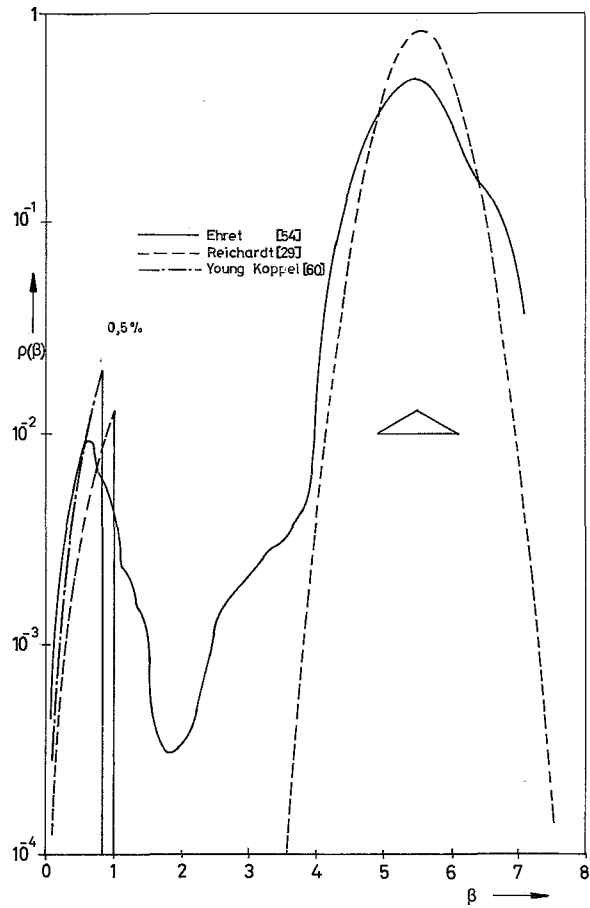


Fig.11 Frequency distributions for zirconium hydride

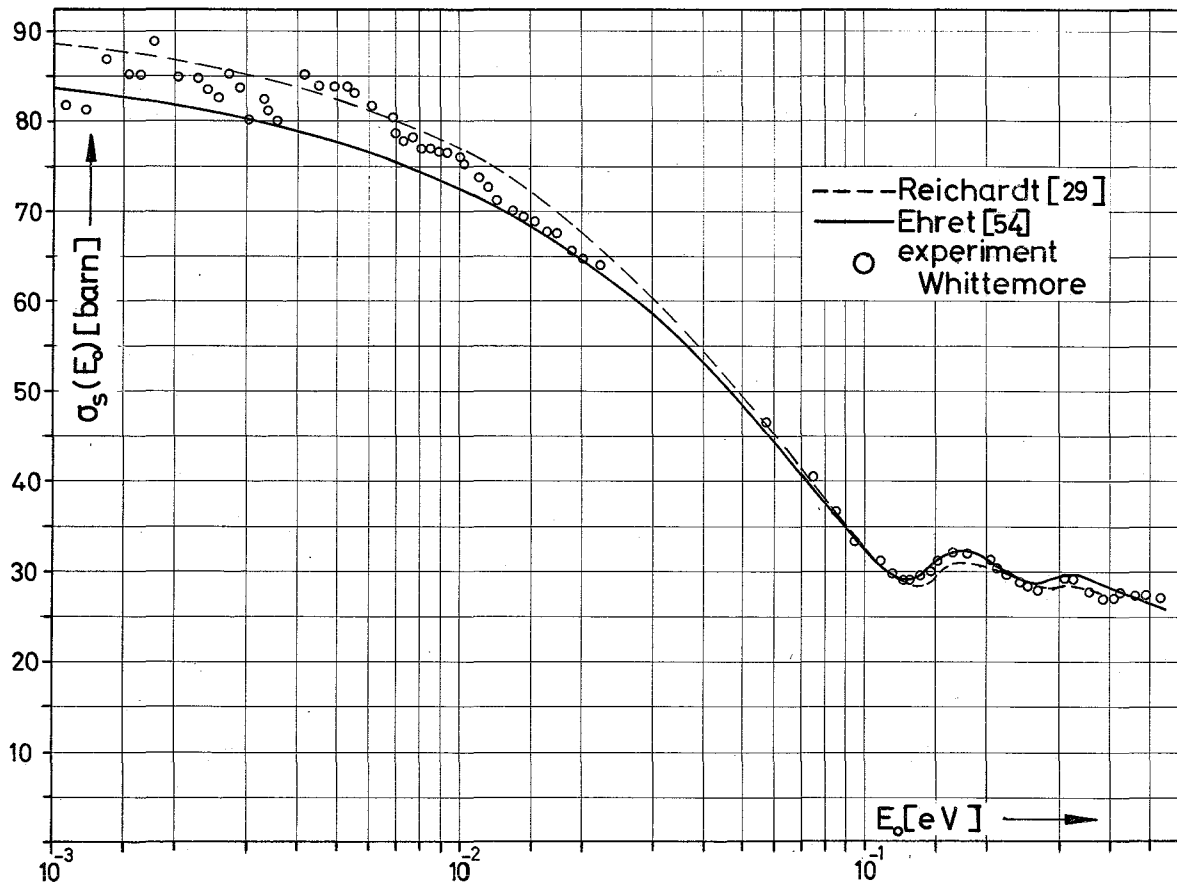
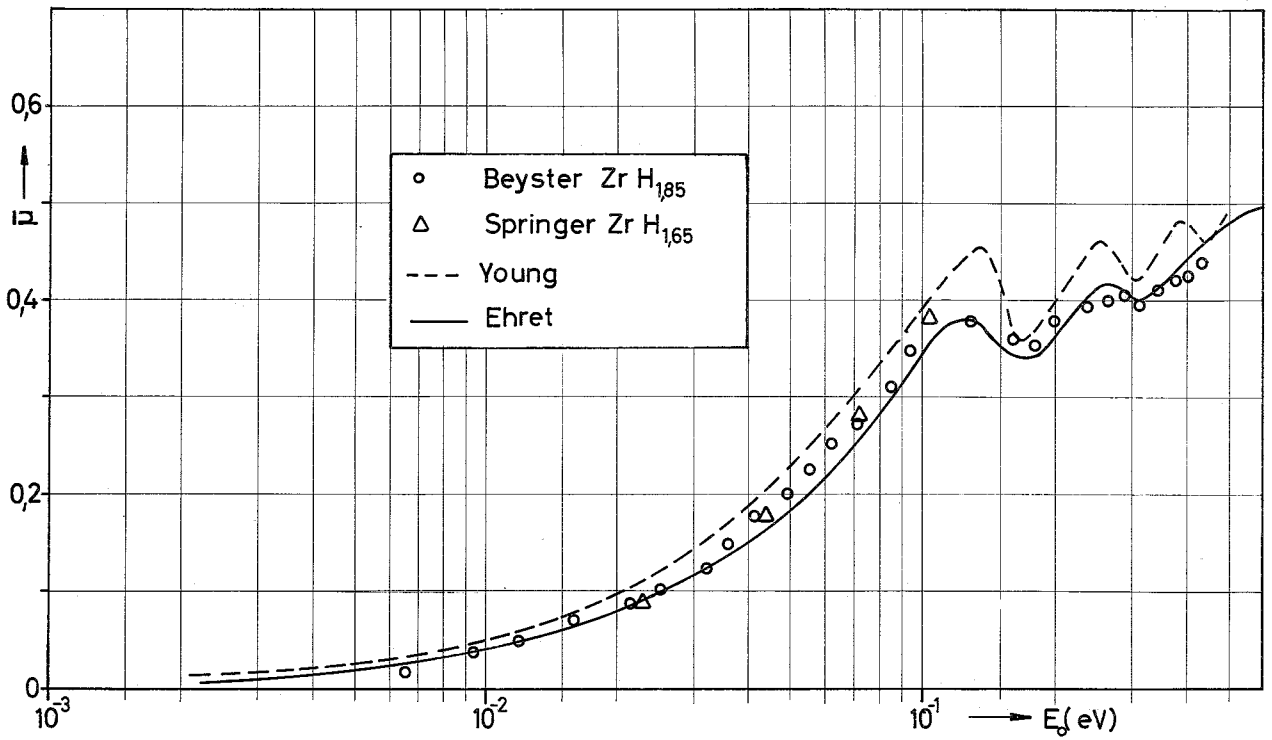
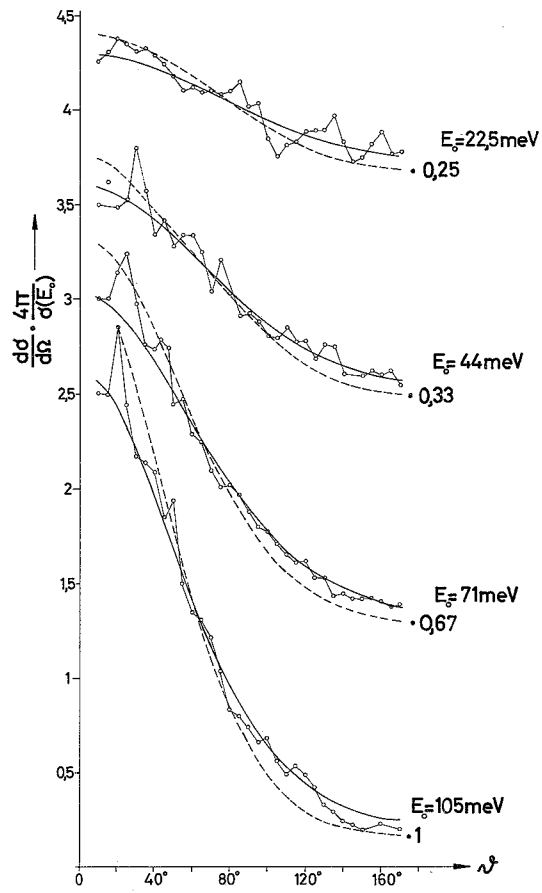


Fig.12 Total cross section of zirconium hydride



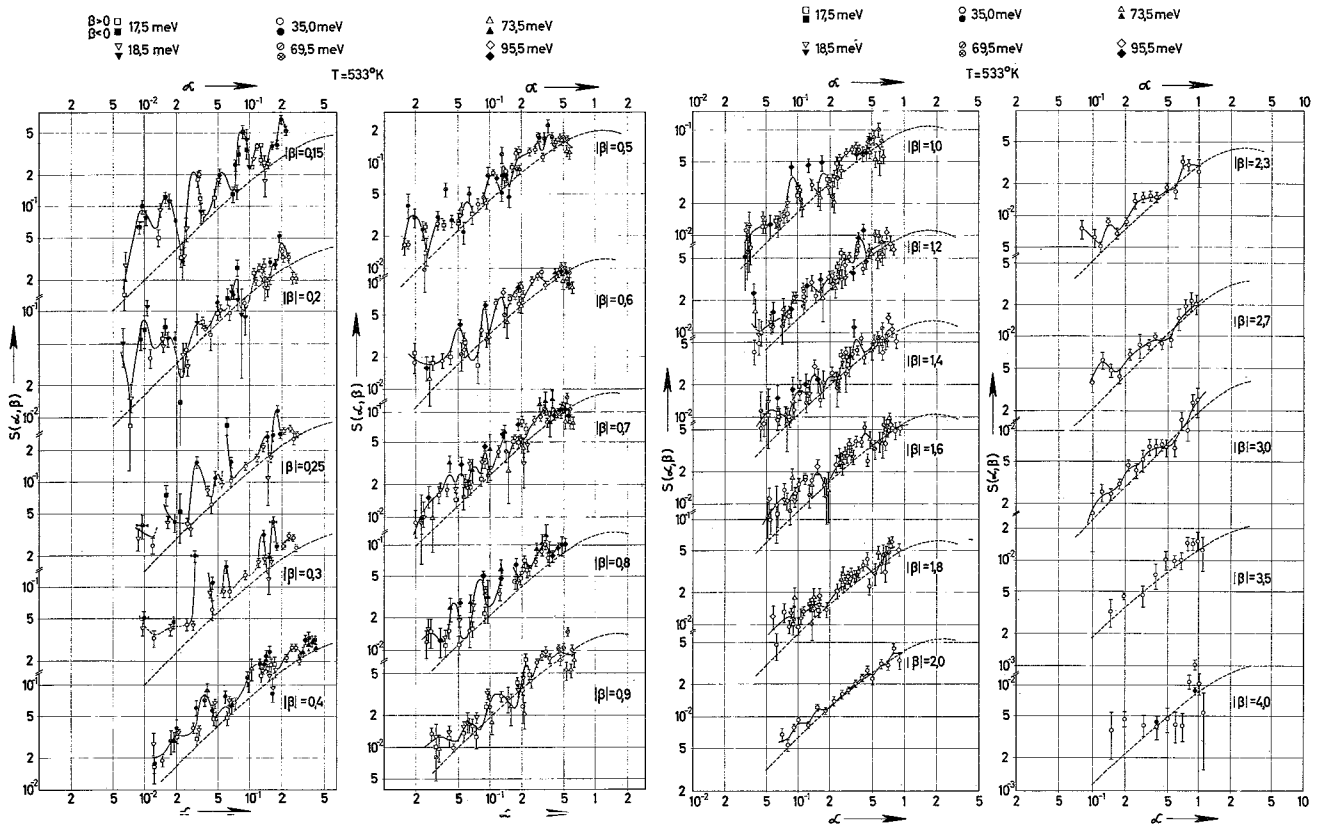


Fig.15 Scattering law $S(\alpha, \beta)$ for graphite at $T=533^\circ\text{K}$

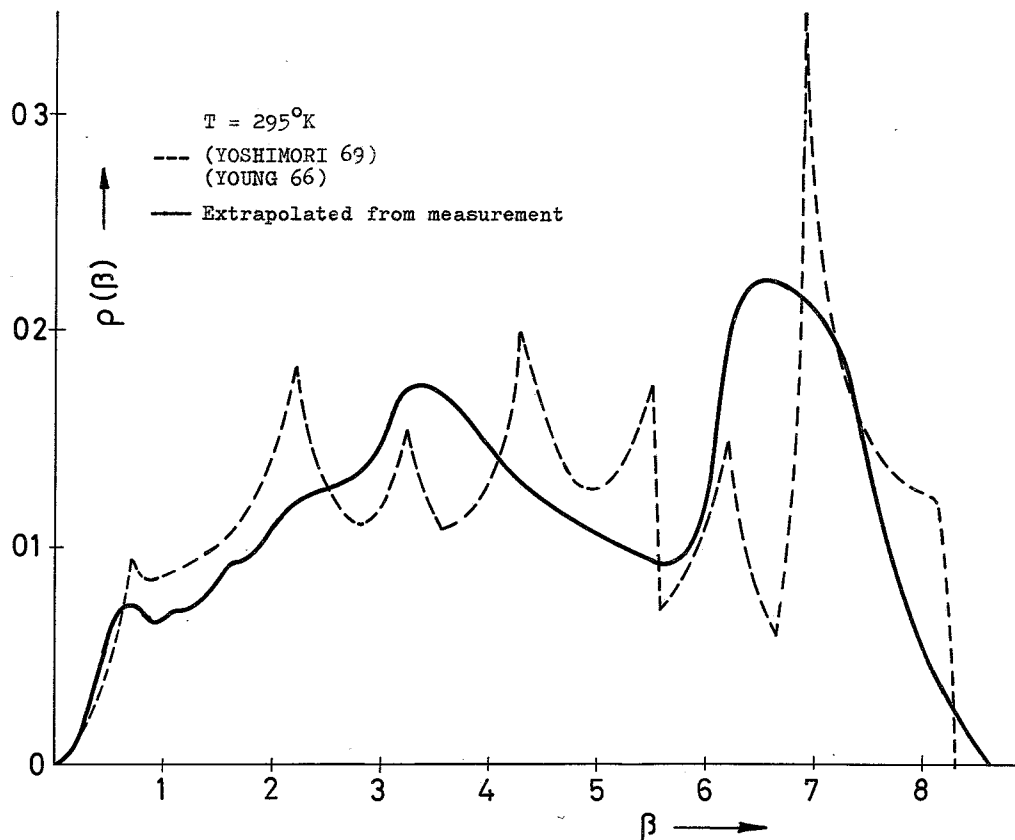


Fig. 16 Frequency distribution of graphite

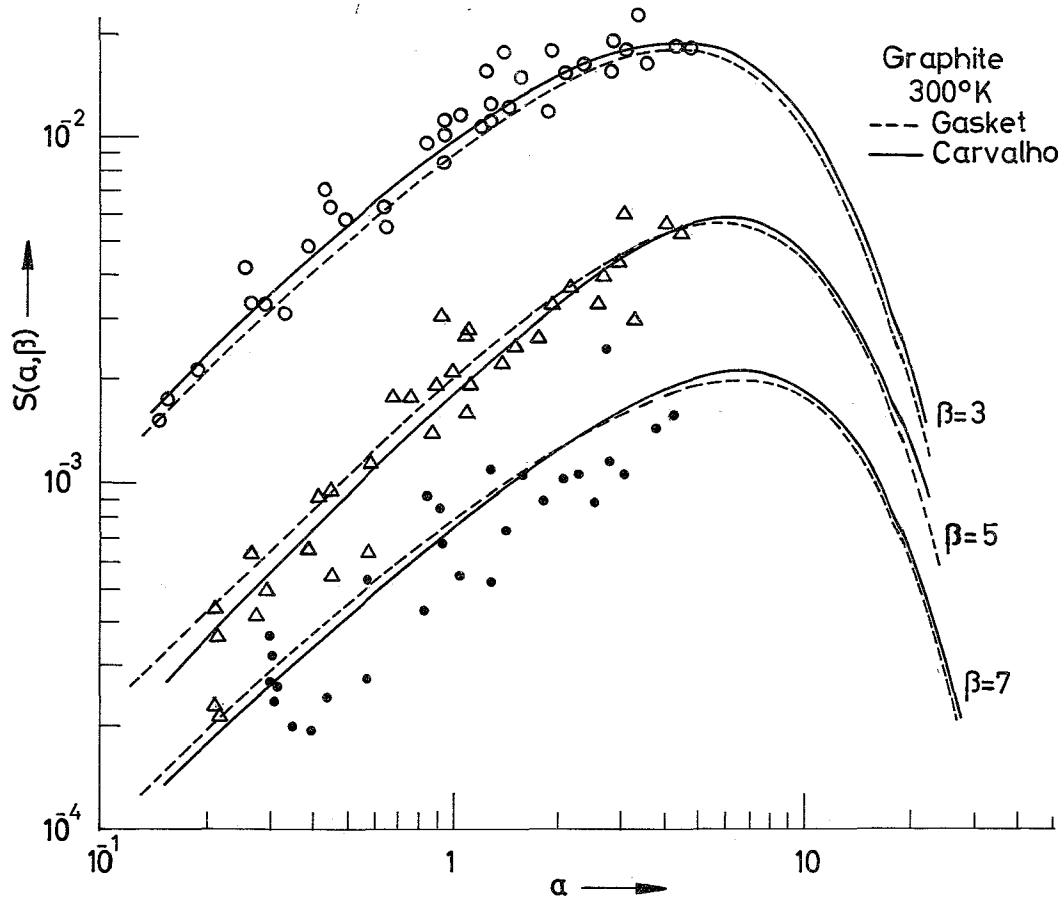


Fig. 17 $S(\alpha, \beta)$ for graphite at high α and β values /67/

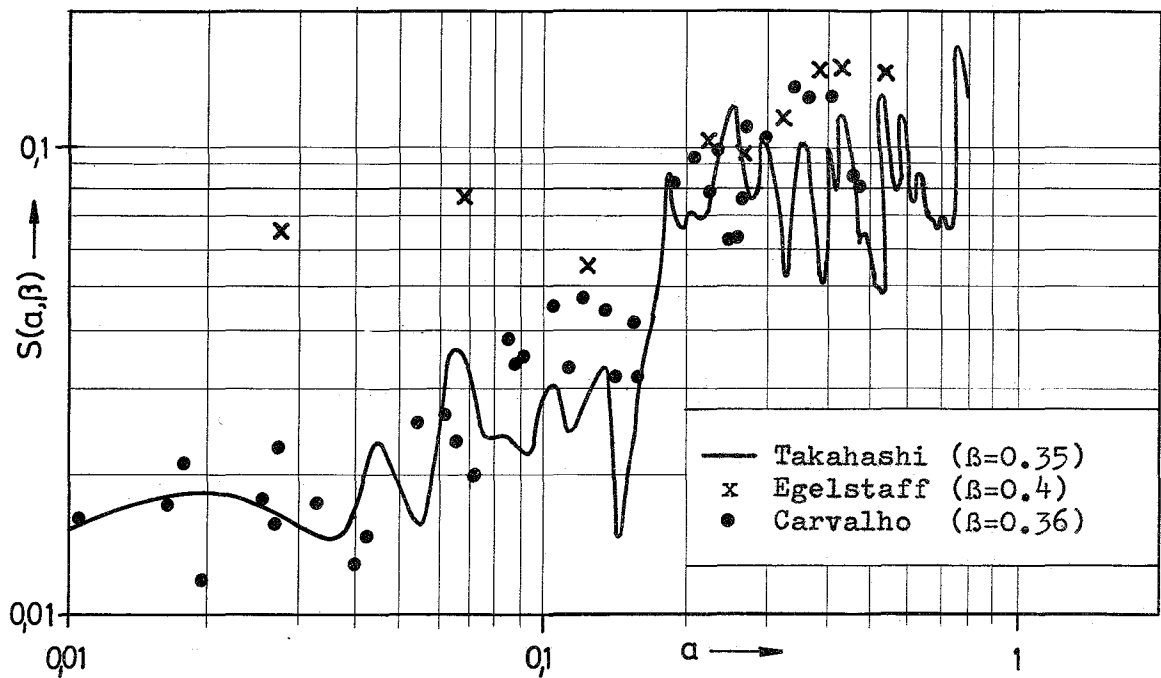


Fig. 18 Coherent one phonon contribution to $S(\alpha, \beta)$

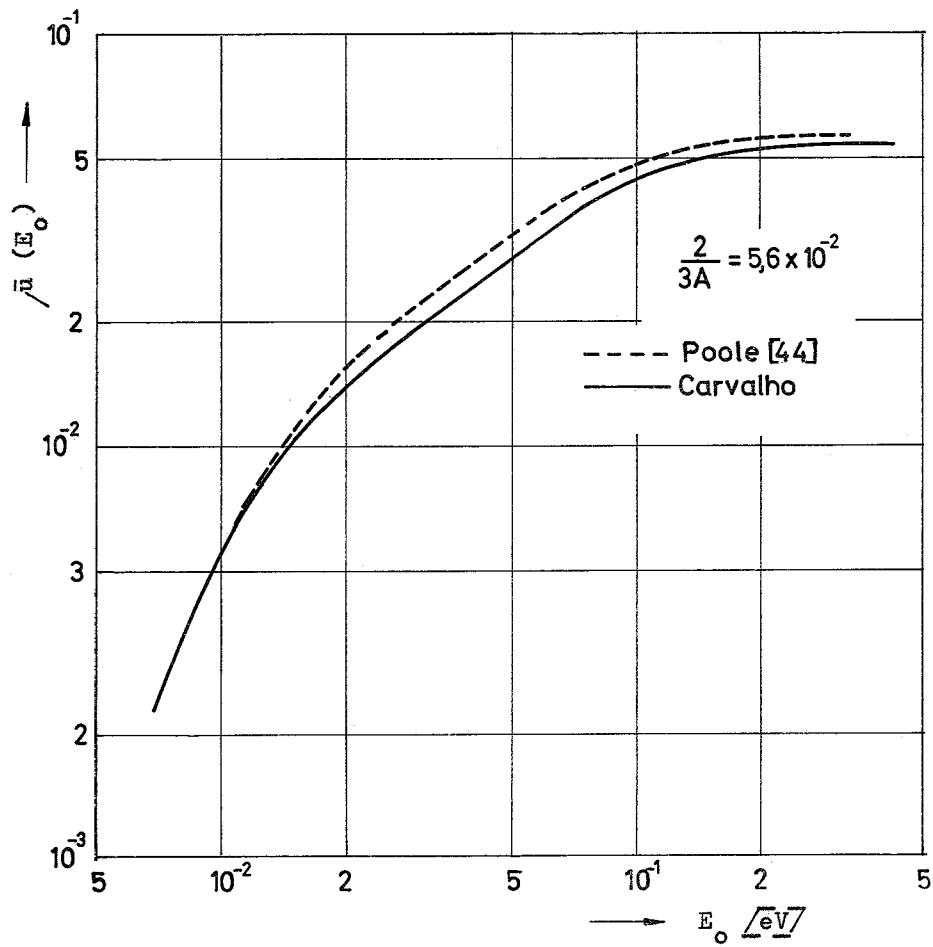


Fig. 19 Average cosine $\bar{\mu}(E_0)$ of graphite

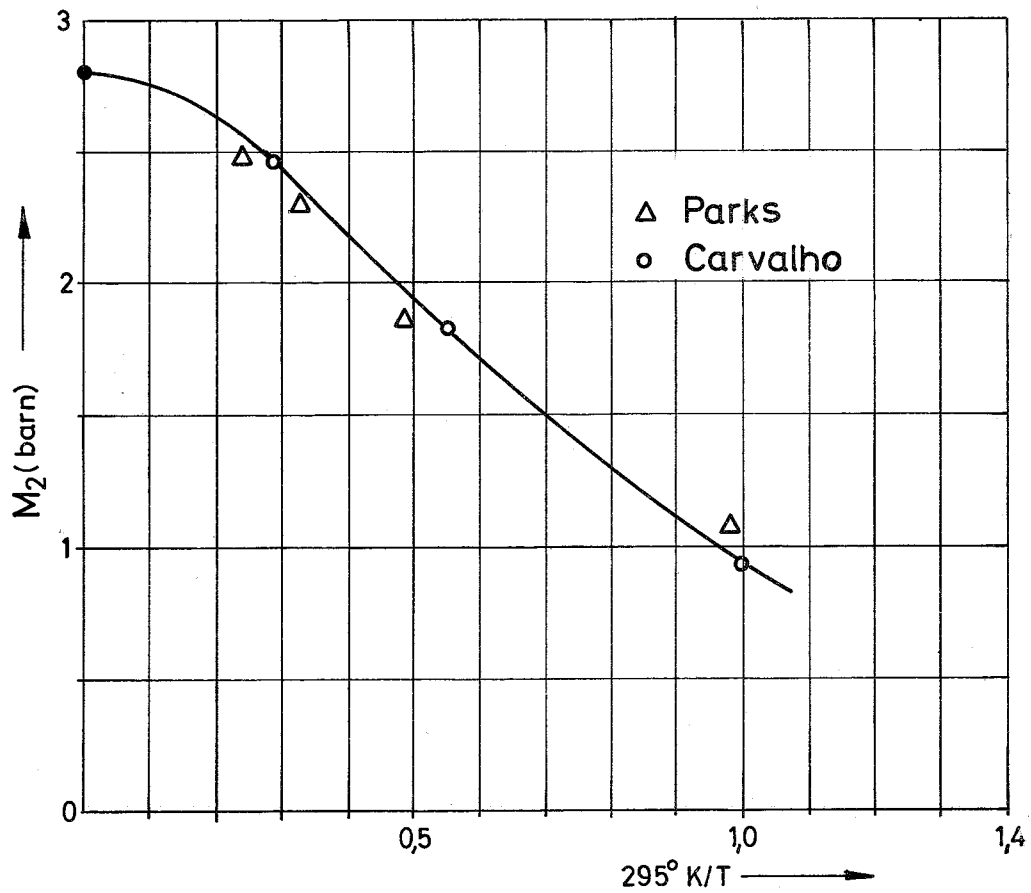


Fig. 20 M_2 for graphite (● free gas)